

Selectivity Estimation with Deep Likelihood Models

Zongheng Yang^{1*}, Eric Liang¹, Amog Kamsetty¹, Chenggang Wu¹, Yan Duan³,
Xi Chen^{1,3}, Pieter Abbeel^{1,3}, Joseph M. Hellerstein¹, Sanjay Krishnan², Ion Stoica¹

¹UC Berkeley ²University of Chicago ³covariant.ai

ABSTRACT

Selectivity estimation has long been grounded in statistical tools for density estimation. To capture the rich multivariate distributions of relational tables, we propose the use of a new type of high-capacity statistical model: deep likelihood models. However, direct application of these models leads to a limited estimator that is prohibitively expensive to evaluate for range and wildcard predicates. To make a truly usable estimator, we develop a Monte Carlo integration scheme on top of likelihood models that can efficiently handle range queries with dozens of filters or more.

Like classical synopses, our estimator summarizes the data without supervision. Unlike previous solutions, our estimator approximates the joint data distribution without any independence assumptions. When evaluated on real-world datasets and compared against real systems and dominant families of techniques, our likelihood model based estimator achieves single-digit multiplicative error at tail, a 40–200× accuracy improvement over the second best method, and is space- and runtime-efficient.

1. INTRODUCTION

Estimating the selectivity of a SQL predicate is a core primitive in query optimization [46], approximate query processing [2], and performance profiling [3]. The main task is to estimate the fraction of a relation that satisfies a predicate, without actual execution. Despite its importance, there is wide agreement that the problem is still unsolved [28, 30, 39]. Open-source and commercial DBMSes routinely produce up to 10^4 – 10^8 × estimation errors on queries over a large number of attributes [28].

The fundamental difficulty of selectivity estimation comes from condensing information about data into summaries [20]. The predominant approach in database systems today is to collect single-column summaries (e.g., histograms and sketches), and to combine these coarse-grained models assuming column independence. This represents one extreme, where the summaries are fast to construct and cheap to store, but compounding errors occur due to the coarse information and over-simplifying independence assumptions. On the other end of the spectrum, when given the *joint data distribution* of a relation (the frequency of each unique tuple normalized by the relation’s cardinality), perfect selectivity “estimates” can be read off or computed via integration over the distribution. However, the *joint* is intractable to compute or store for all but the tiniest datasets. Thus, tradi-

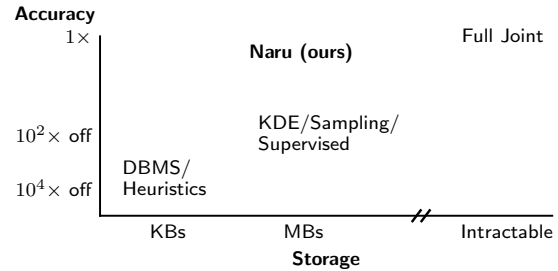


Figure 1: Approximating the joint data distribution in full, Naru enjoys high space efficiency and estimation accuracy.

tional selectivity estimators are faced with the hard tradeoff between the amount of information captured and the cost to construct, store, and query the summary.

An accurate and compact *joint approximation* would largely dispense with this tradeoff (Figure 1). Recent advances in unsupervised learning have offered promising tools in this regard. While it was previously thought intractable to approximate the joint data distribution of a relation in its full form [8, 14], *deep likelihood models*, a type of density estimator, have succeeded in modeling high-dimensional data such as images, text, and audio [44, 52–54]. However, these models only estimate *point densities*—in query processing terms, they only handle equality predicates (“what is the fraction of tuples with price equal to \$100?”). Full-featured selectivity estimation requires handling not only equality but also range predicates (“what fraction of tuples have price less than \$100 and weight greater than 10lbs?”). Naive estimation of the range density by integrating over the query region requires summing up an enormous number of points. In an 11-dimensional table we consider, a challenging range query has 10^{10} points in the query region, which would take more than 1,000 hours to sum over by a naive enumeration scheme. A full-featured selectivity estimator, therefore, requires new techniques beyond the state of the art.

In this paper, we show how selectivity estimation can be done with high accuracy by using *deep likelihood models*. We show how relational data—including both numeric and categorical attributes—can be mapped into these models for effective selectivity estimation of equality predicates. We then introduce a new Monte Carlo integration technique called *progressive sampling*, which efficiently estimates range queries even at high dimensionality. By leveraging the availability of conditional probability distributions provided by the model, progressive sampling steers the sampler into regions of high probability density, and then corrects for the

*Correspondence to: zongheng@berkeley.edu.

induced bias by using importance weighting. This technique extends the state of the art in density estimation, with particular applicability to our problem of general-purpose selectivity estimation. Our scheme is effective: a thousand samples suffice to accurately estimate the aforementioned 10^{10} -point query.

To realize these ideas, we design and implement **Naru** (**N**eural **R**elation **U**nderstanding), a selectivity estimator that approximates the joint data distribution in its full form, without any column independence assumptions. Approximating the joint in full not only provides superior accuracy, but also frees us from specifying what combinations of columns to build synopses on. We further propose optimizations to encode and decode a wide spectrum of characteristics in real-world relational data (e.g., various datatypes, small vs. large domain sizes). Combining our integration scheme with these practical strategies results in a highly accurate, compact, and functionality-rich selectivity estimator based on deep likelihood models.

Just like classical synopses, **Naru** summarizes a relation in an unsupervised fashion. The model is trained via statistically grounded principles (maximum likelihood) where no supervised signals or query feedback are required. While many *query-driven* estimators are concerned with optimizing with respect to a set of training queries (i.e., “how much error does the estimator incur on these queries?”), **Naru** is optimized with respect to the underlying data distribution (i.e., “how divergent is the estimator from the data?”). Our full joint approximation is orthogonal to query-driven approaches: an unsupervised likelihood model can always take advantage of additional signals such as query feedback by further fine-tuning. On the other hand, being data-driven, **Naru** supports a much larger set of queries and is automatically robust to query distributional shifts. Our evaluation compares **Naru** to the state-of-the-art unsupervised and supervised techniques, showing **Naru** to be the only estimator to achieve worst-case *single-digit multiplicative errors* for challenging high-dimensional queries.

This paper makes three principal contributions:

1. We show how deep likelihood models can be used for selectivity estimation (§2, §3), and propose optimizations to make them suitable for relational data (§4).
2. We identify range query estimation to be the key challenge for likelihood model-based selectivity estimators. To address this challenge, we develop *progressive sampling*, a Monte Carlo integration technique that efficiently estimates range densities even with large query regions (§5).
3. Our estimator **Naru**, when evaluated on several real-world datasets and compared to baseline of different families (heuristics, real DBMSes, statistical methods, supervised learning), achieves orders-of-magnitude better accuracy with space usage $\sim 1\%$ of data size and $\sim 10\text{ms}$ of estimation latency (§6).

2. PROBLEM FORMULATION

Consider a relation T with attribute domains $\{A_1, \dots, A_n\}$. Selectivity estimation seeks to estimate the fraction of tuples in T that satisfy a particular predicate, $\theta : A_1 \times \dots \times A_n \rightarrow \{0, 1\}$. We define the selectivity to be $\text{sel}(\theta) := |\{\mathbf{x} \in T : \theta(\mathbf{x}) = 1\}|/|T|$.

The *joint data distribution* of the relation, defined to be

$$P(a_1, \dots, a_n) := f(a_1, \dots, a_n)/|T|$$

is closely related to the selectivity, where $f(a_1, \dots, a_n)$ is the number of occurrences of tuple (a_1, \dots, a_n) in T . It forms a valid probability distribution since integrating it over the attribute domains yields a value of 1. Thus, exact selectivity calculation is equivalent to integration over the joint:

$$\text{sel}(\theta) = \sum_{a_1 \in A_1} \dots \sum_{a_n \in A_n} \theta(a_1, \dots, a_n) \cdot P(a_1, \dots, a_n).$$

In this work, we consider the relation T finite and hence its empirical domains A_i are finite. Thus, summation is used in the integration calculation above.

2.1 Approximating the Joint via Factorization

Given the joint, exact selectivity “estimates” can be calculated by integration. However, the number of entries in the joint—and thus the maximum number of points needed to be summed over in the integration—is

$$|P| = \prod_{i=1}^n |A_i|$$

a size that grows exponentially with the number of attributes. Although small-domain categorical columns, e.g., record types, do exist, large-domain columns or wide tables are common, rendering the calculation or storage of the true joint intractable. Real-world tables with a dozen or so columns can easily have a joint size of 10^{20} and upwards (§6). Thus, joint approximation techniques seek to *factorize* [15] the joint into some lower-dimensional representation, $\hat{P} \approx P$, for practical construction, storage, and query.

Classical 1D histograms [46] use the simplest factorization

$$\hat{P}(a_1, \dots, a_n) \approx \prod_{i=1}^n \hat{P}(a_i)$$

where independence between attributes is assumed. The $\hat{P}(a_i)$ ’s are materialized as histograms that are now cheap to construct and store. Selectivity estimation reduces to calculating per-column selectivities and combining by multiplication,

$$\text{sel}(\theta) \approx \left(\sum_{a_1 \in A_1} \theta_1(a_1) \hat{P}(a_1) \right) \times \dots \times \left(\sum_{a_n \in A_n} \theta_n(a_n) \hat{P}(a_n) \right)$$

where each θ_i is predicate θ projected to each attribute (assuming here θ is a conjunction of single-attribute filters).

Richer factorizations are possible and are generally more accurate approximations to the joint. For instance, Probabilistic Relational Models [13,14] from the early 2000s leverage the conditional independence assumptions of Bayesian Networks (e.g., joint factored into $\{\hat{P}(a_1|a_2, a_3), \hat{P}(a_2), \hat{P}(a_3)\}$). Dependency-Based Histograms [8] use decomposable interaction models and rely on partial independence between columns (e.g., $\hat{P}(a_1, a_2, a_3) \approx \hat{P}(a_1)\hat{P}(a_2, a_3)$). Both methods are marked improvements over 1D histograms since they capture more than single-column interactions. However, the tradeoff between richer factorizations and costs to store or integrate is still unresolved. The above parametric factors are materialized either as probability tables or as histograms, thus the cost of construction and storage grows

large for a large number of attributes. Obtaining selectivities also becomes drastically harder due to the integration now crossing multiple attribute domains. Lastly, the approximated joint’s precision is compromised since some forms of independence are still assumed.

In this paper, we consider the richest possible factorization of the joint, using the chain rule:

$$\hat{P}(a_1, \dots, a_n) = \hat{P}(a_1)\hat{P}(a_2|a_1)\cdots\hat{P}(a_n|a_1, \dots, a_{n-1})$$

Unlike the previous proposals, the chain rule factorization is an *exact* relationship to represent a distribution. It makes no independence assumptions and captures all complex interactions between attributes. Key to this goal is that the factors, $\{\hat{P}(a_i|a_1, \dots, a_{i-1})\}$, need not be materialized; instead, they are calculated on-demand by a neural network, a high-capacity universal function approximator [11].

2.2 Problem Statement

This paper considers estimating the selectivities of queries consisting of conjunctions of range/equality predicates on numeric and categorical attributes (e.g., strings, dates, bools), each of which involving an attribute and a literal. We assume the *domain* of each column, A_i , is finite: since a real dataset is finite, we can take the actually present values of a column as its finite domain.

We make a few remarks. First, the supported queries are wide: the usual $=, \neq, <, \leq, >, \geq$ operators, the rectangular containment $A_i \in [l_i, r_i]$, or even the IN operator are considered ranges under our formulation. Arbitrary conjunctions or disjunctions of such operators are supported via the inclusion-exclusion principle. Second, our formulation follows a large amount of existing work on this topic [8,14,19,38,41] and, in some cases, offers more capabilities (e.g., certain prior work require each predicate be a rectangle [19,25], columns be real-valued [19,26], or assume equality predicates only [17]). Third, similar to prior work, the relation under estimation can either be a base table or a join result.

3. DEEP LIKELIHOOD MODELS

3.1 Overview

Naru uses a deep likelihood model to provide an accurate estimate of the joint distribution, \hat{P} . We overview two categories of such models and discuss the subset suitable for a selectivity estimator.

Access to point density $\hat{P}(\mathbf{x})$. All deep likelihood models can produce point density estimates $\hat{P}(\mathbf{x})$ after training on a set of n -dimensional tuples $T = \{\mathbf{x}_1, \dots\}$ with the unsupervised maximum likelihood objective. Many network architectures have been proposed, ranging from latent variable models [24], normalizing flows [9,23], to autoregressive models such as masked multi-layer perceptrons (MLP) [12,51] and the Transformer [54].

Access to autoregressive densities $\{\hat{P}(x_i|\mathbf{x}_{<i})\}$. A subclass of models, termed *autoregressive models*, provides access to the conditional densities present in the chain rule:

$$\begin{aligned} \hat{P}(\mathbf{x}) &= \hat{P}(x_1, x_2, \dots, x_n) \\ &= \hat{P}(x_1)\hat{P}(x_2|x_1)\cdots\hat{P}(x_n|x_1, \dots, x_{n-1}) \end{aligned}$$

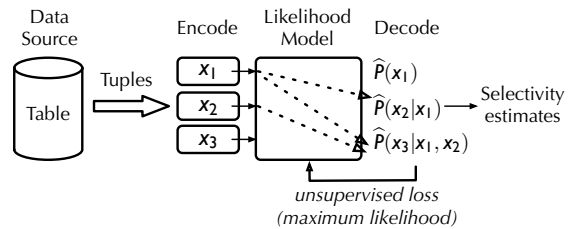


Figure 2: **Overview of the estimator framework.** Like classical synopses, Naru reads data tuples and does not require supervised training queries or query feedback. The pluggable likelihood model (§3.2), encoding/decoding strategies (§4.2), and querying algorithms (§5) are shown.

Namely, given input tuple $\mathbf{x} = (x_1, \dots, x_n)$, the model emits n conditional density estimates, $\{\hat{P}(x_i|\mathbf{x}_{<i})\}$. These estimates offer a finer resolution than a single point density scalar. The model can be architected to use any ordering(s) of the attributes (e.g., (x_1, x_2, x_3) or (x_2, x_1, x_3)); in this work we simply pick the table order.

Naru’s core consists of a configurable autoregressive model. At first glance, the additional conditionals may not seem to benefit our selectivity estimation task, but there are two important reasons this family of models is the right choice.

First, autoregressive models have shown superior modeling precision than other types of likelihood models (e.g., flows) in modeling images [44,53], audios [52], and text [54]. All these problems have high-dimensional data akin to a relational table. Second, as will be seen in §5.1, the conditional densities are critical in supporting range query estimation, a feature not possible with access to point densities only.

3.2 Autoregressive Models for Relational Data

Naru allows any autoregressive model \mathcal{M} to be plugged in, as long as it satisfies the following form:

$$\mathcal{M}(\mathbf{x}) \mapsto [\hat{P}(X_1), \hat{P}(X_2|x_1), \dots, \hat{P}(X_n|x_1, \dots, x_{n-1})] \quad (1)$$

Namely, one tuple goes in, a list of conditional density distributions comes out, each being a *distribution* of the i th attribute conditioned on previous attributes. *Scalars* $\{\hat{P}(x_i|\mathbf{x}_{<i})\}$ are read off from them. How can a neural net \mathcal{M} ensure this autoregressive property, e.g., making sure $\hat{P}(X_3|x_1, x_2)$ only depends on, or “sees”, the information from the first two attribute values (x_1, x_2) but not anything else?

The machine learning community has investigated many such autoregressive architectures, both general-purpose [12,54], and specialized for domains such as images [53]. Here, we propose an architecture suitable for modeling relational data. The basic building block is to assign each column i its own compact neural net, whose input is the aggregated information about *previous* column values $\mathbf{x}_{<i}$. Its role is to use this context information to output a distribution over its own domain, $\hat{P}(X_i|\mathbf{x}_{<i})$. Consider a `travel_checkins` table from an online maps app with columns `city`, `year`, `stars`. Suppose the input is tuple `(Portland, 2017, 10)`. First, column-specific encoders $E_{col}()$ transform each attribute value into a numeric vector suitable for neural net consumption,

$$[E_{city}(\text{Portland}), E_{year}(2017), E_{stars}(10)]$$

Then, feed appropriately aggregated encoded input to the

per-column neural nets \mathcal{M}_{col} :

$$\begin{aligned} \mathbf{0} &\rightarrow \mathcal{M}_{\text{city}} \\ E_{\text{city}}(\text{Portland}) &\rightarrow \mathcal{M}_{\text{year}} \\ \oplus (E_{\text{city}}(\text{Portland}), E_{\text{year}}(2017)) &\rightarrow \mathcal{M}_{\text{stars}} \end{aligned}$$

where \oplus is the operator that aggregates information from several encoded attributes. In practice, this aggregator can be vector concatenation, a set-invariant *pooling* operator (e.g., elementwise sum or max), or even self-attention [54].

Notice that the first output, from $\mathcal{M}_{\text{city}}$, does not depend on any attribute values (its input $\mathbf{0}$ is arbitrarily chosen). The second output depends only on the attribute value from *city*, and the third depends only on both *city* and *year*. Therefore, the three outputs can be interpreted as

$$\left[\hat{P}(\text{city}), \hat{P}(\text{year}|\text{city}), \hat{P}(\text{stars}|\text{city}, \text{year}) \right]$$

Thus, autoregressiveness is achieved.

Training these model outputs to be as close as possible to the true conditional densities is done via maximum likelihood estimation. Specifically, the *cross entropy* measure [11] between the true data joint P and the model estimate \hat{P} is calculated over all tuples in relation T and used as the loss:

$$\mathcal{H}(P, \hat{P}) = - \sum_{\mathbf{x} \in T} P(\mathbf{x}) \log \hat{P}(\mathbf{x}) = - \frac{1}{|T|} \sum_{\mathbf{x} \in T} \log \hat{P}(\mathbf{x}) \quad (2)$$

It can be fed into a standard gradient descent optimizer [22].

3.3 Interpreting Goodness-of-Fit: Entropy Gap

Like any statistical distribution estimators, our choice of deep likelihood models admits an interpretable goodness-of-fit. The cross entropy measure (Equation 2) and the entropy of the data, $\mathcal{H}(P)$, satisfy the relationship:

$$\mathcal{H}(P, \hat{P}) - \mathcal{H}(P) = D_{\text{KL}}(P \parallel \hat{P})$$

where $D_{\text{KL}}(P \parallel \hat{P})$ is the Kullback-Leibler divergence (KL) measure quantifying how different the model’s approximate distribution \hat{P} is from the true distribution P . The measure is non-negative and zero implies a perfect fit. If data entropy $\mathcal{H}(P)$ is calculable (i.e., the data is static), then during and after training, one can monitor the KL divergence, or *entropy gap* in bits, as the interpretable goodness-of-fit.

4. ESTIMATOR CONSTRUCTION

We now discuss practical issues in constructing Naru.

4.1 Workflow

Figure 2 outlines the workflow of building a Naru estimator. After specifying a table T to build an estimator on, batches of random tuples from T are read to train Naru. In practice, a snapshot of the table can be saved to external storage so normal DBMS activities are not affected. Neural network training can be performed either close to the data (at periods of low activity) or offloaded to a remote process.

For a batch of tuples, Naru encodes each attribute value using column-specific strategies (§4.2). The encoded batch then gets fed into the model to perform a gradient update step. Our evaluation (§6.4) empirically observed that one pass over data is sufficient to achieve a high degree of accuracy (e.g., outperforming real DBMSes by 10–20×), and more passes are beneficial until model convergence.

Data appends and updates, however, may cause statistical staleness. Naru can be periodically fine-tuned on samples from the updated relation to correct for this, as we show in §6.7.3. We note that update handling is a concern shared by many classical synopses, and that Naru can leverage system-level techniques for handling updates from the literature (e.g., partitioning and periodic bulk updates).

Joins. The estimator does not distinguish between the type of table it is built on. To build an estimator on a joined relation, either the entire joined relation can be pre-computed and materialized, or multi-way join operators [55,56] and samplers [5,29] can be used to produce batches of tuples on-the-fly. Given access to tuples from the joined result, no changes are needed to the estimator framework. Once trained, the estimator supports queries that filter any column in the joined relation. This treatment follows prior work [21,33,38] and is conceptually clean.

4.2 Encoding and Decoding Strategies

Naru models a relation as a high-dimensional discrete distribution. The key challenge is to *encode* each column into a form suitable for neural network consumption, while preserving the column semantics. Further, each column’s output distribution $\hat{P}(X_i|\mathbf{x}_{<i})$ (a vector of scores) must be efficiently *decoded* regardless of its datatype or domain size.

For each column Naru first obtains its domain A_i either from user annotation or by scanning. All values in the column are then dictionary-encoded into integer IDs in range $[0, |A_i|)$. For instance, the dictionary can be $\text{Portland} \mapsto 0$, $\text{SF} \mapsto 1$, etc. For columns with a natural order, e.g., numerics or strings, the domains are sorted to make the dictionary order consistent with the column order. Note that continuous datatypes are discretized the same way. A special placeholder \perp can be inserted into the domain so that a previously-built estimator can function on new data.

Next, column-specific encoders $E_{\text{col}}()$ encode these IDs into vectors. The ML community has proposed many such strategies before; we make sensible choices by keeping in mind a few characteristics specific to relational datasets:

Encoding small-domain columns: one-hot. For such a column $E_{\text{col}}()$ is set to *one-hot encoding* (i.e., indicator variables). For instance, if there are a total of 4 cities, then the encoding of SF is $E_{\text{city}}(1) = [0, 1, 0, 0]$, a 4-dimensional vector. The small-domain threshold is configurable and set to 64 by default. This encoding takes $O(|A_i|)$ space.

Encoding large-domain columns: embedding. For a larger domain, the one-hot vector wastes space and computation budget. Naru uses embedding encoding in this case. In this scheme—a preprocessing step in virtually all natural language processing tasks—a learnable embedding matrix of type $\mathbb{R}^{|A_i| \times h}$ is randomly initialized, and $E_{\text{col}}()$ is simply row lookup into this matrix. For instance, $E_{\text{year}}(4) \mapsto$ row 4 of embedding matrix, an h -dimensional vector. The embedding matrix gets updated during gradient descent as part of the model weights. This encoding takes $O(h)$ space, independent of the domain size (Naru defaults h to 64). This encoding is ideal for domains with a meaningful semantic distance (e.g., cities are similar in geo-location, popularity, relation to its nation) since each dimension in the embedding vector can learn to represent each such similarity.

(Easy) Decoding small-domain columns. Suppose domain $|A_i|$ is small. In this easy case, the network allocates an *output layer* to compute a *distribution* $\hat{P}(X_i|\mathbf{x}_{<i})$, which is a $|A_i|$ -dimensional vector of probabilities used for selectivity estimation. The output layer may be a fully connected layer, $\text{FC}(F, |A_i|)$, where F is the hidden unit size. For example, for a city column with three values in its domain, the output distribution may be [SF = 0.2; Portland = 0.5; Waikiki = 0.3]. During optimization, the training loss seeks to minimize the divergence of this output from the true data distribution.

(Harder) Decoding large-domain columns: embedding reuse. If the domain is large, however, using an output layer $\text{FC}(F, |A_i|)$ would be inefficient in both space and compute. Indeed, an *id* column in a dataset we tested on has a large domain size of $|A_i| = 10^4$, inflating the output layer beyond typical scales.

Naru solves this problem by an optimization that we call “embedding reuse”. In essence, we replace the potentially large output layer $\text{FC}(F, |A_i|)$ with a much smaller version, $\text{FC}(F, h)$ (recall that h is the typically small embedding dimensions; defaults to 64). This immediately yields a saving ratio of $\frac{|A_i|}{h}$. The goal of decoding is to take in inputs $\mathbf{x}_{<i}$ and output $|A_i|$ probability scores over the domain. With the shrunk-down output layer, inputs $\mathbf{x}_{<i}$ would pass through the net arriving at an h -dimensional feature vector, $H \subseteq \mathbb{R}^{1 \times h}$. We then calculate HE_i^T , where $E_i \subseteq \mathbb{R}^{|A_i| \times h}$ is the *already-allocated* embedding matrix for column i , obtaining a vector $\mathbb{R}^{1 \times |A_i|}$ that can be interpreted as the desired scores after normalization. We have thus decoded the output while cutting down the cost of compute and storage. This scheme has proved effective in other large-domain tasks [43].

4.3 Model Choice

As discussed, any autoregressive model can be plugged in, taking advantage of Naru’s encoding/decoding optimizations as well as querying capabilities (§5). We provide two implementations to choose from: (A) the architecture outlined in §3.2 and (B) a masked autoencoder [12] (a basic multi-layer perceptron with similar information-limiting to ensure autoregressiveness). On a 15-column dataset we evaluated on, when controlling for the same parameter count, architecture A achieves better quality than B (8% better entropy gap; §3.3). The same trend holds on another dataset. However, architecture B’s current implementation is more optimized. Naru therefore defaults to architecture B over better learning quality and faster convergence. We defer the study of all possible model choices to future work.

5. QUERYING THE ESTIMATOR

Once a likelihood model is constructed, it can be queried to compute selectivity estimates. Assume a query $\text{sel}(\theta) = P(x_1 \in R_1, \dots, x_n \in R_n)$ asking for the selectivity of the conjunction, where each range R_i can be a point (equality predicate), an interval (range predicate), or any subset of the domain (IN). The calculation of this density is fundamentally summing up the probability masses distributed in the cross-product region, $R = R_1 \times \dots \times R_n$.

We first discuss the straightforward support for equality predicates, then move on to how Naru solves the more challenging problem of range predicates.

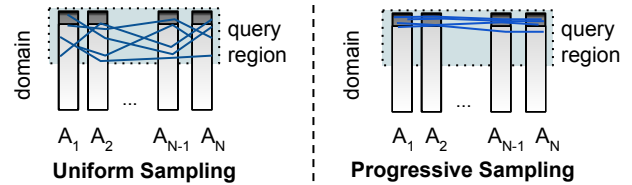


Figure 3: **Intuition of progressive sampling.** Uniform samples taken from the query region have a low probability of hitting the high-mass sub-region of the query region, increasing the variance of Monte Carlo estimates. Progressive sampling avoids this by sampling from the estimated data distribution instead, which naturally concentrates samples in the high-mass sub-region.

Equality Predicates. When values are specified for *all* columns, estimating conjunctions of these equality predicates is straightforward. Such a point query has the form $P(X_1 = x_1, \dots, X_n = x_n)$ and requires only a single forward pass on the point, (x_1, \dots, x_n) , to obtain the sequence of conditionals, $[\hat{P}(X_1 = x_1), \hat{P}(X_2 = x_2|X_1 = x_1), \dots, \hat{P}(X_n = x_n|X_1 = x_1, \dots, X_{n-1} = x_{n-1})]$, which are then multiplied.

Range Predicates. It is impractical to assume a workload that only issues point queries. With the presence of any range predicate, or when some columns are not filtered, the number of points that must be evaluated through the model becomes larger than 1. (In fact, it easily grows to an astronomically large number for the majority of workloads we considered.) We discuss two ways in which Naru carries out this operation. *Enumeration* exactly sums up the relevant model densities: when the queried region R is sufficiently small, all discrete points in this region are enumerated and fed into the model, in a batching fashion, whose corresponding point densities are then summed up:

$$\text{sel}(X_1 \in R_1, \dots, X_n \in R_n) \approx \sum_{x_1 \in R_1} \dots \sum_{x_n \in R_n} \hat{P}(x_1, \dots, x_n).$$

When the region R is deemed too big—almost always the case in the datasets and workloads we considered—we instead use a novel approximate technique termed *progressive sampling*, an unbiased estimator that works surprisingly well on the relational datasets we considered.

5.1 Range Queries via Progressive Sampling

The queried region $R = R_1 \times \dots \times R_n$ in the worst case contains $O(\prod_i D_i)$ points, where $D_i = |A_i|$ is the size of each attribute domain. Clearly, computing the likelihood for an exponential number of points is prohibitively expensive for data/queries with even moderate dimensions. Naru proposes an approximate integration scheme to address this challenge.

First attempt (Figure 3, left). The simplest way to approximate the sum is via uniform sampling. First, sample $\mathbf{x}^{(i)}$ uniformly at random from R . Then, query the model to compute $\hat{p}_i = \hat{P}(\mathbf{x}^{(i)})$. By naive Monte Carlo, for S samples we have $\frac{|R|}{S} \sum_{i=1}^S \hat{p}_i$ as an unbiased estimator to the desired density. Intuitively, this scheme is randomly throwing points into target region R to probe its average density.

To understand the failure mode of uniform sampling, consider a relation T with n correlated columns, with each column distribution skewed so that 99% of the probability mass is contained in the top 1% of its domain (Fig-

ure 3). Take a query with range predicates selecting the top 50% of each domain. It is easy to see that uniformly sampling from the query region will take in expectation $1/(0.01/0.5)^n = 1/0.02^n$ samples to hit the high-mass region we are integrating over. Thus, the number of samples needed for an accurate estimate increases exponentially with n . Consequently, we find that this sampler collapses catastrophically in the real-world datasets that we consider. For instance, on a relation with $n = 11$ columns, this sampler *almost always* returned density estimates of 0.0 even with thousands of samples per query. Consequently, it had the worst errors among all baselines in our evaluation.

Progressive sampling (Figure 3). Instead of uniformly throwing points into the region, we could be more selective in the points we choose—precisely because we have a powerful likelihood model trained. Intuitively, a sample of the first dimension $x_1^{(i)}$ would allow us to “zoom in” into the *more meaningful region of the second dimension*. This more meaningful region is exactly described by the second conditional output from the likelihood model, $\hat{P}(X_2|x_1^{(i)})$, a distribution over the second domain given the first dimension sample. We can obtain a sample of the second dimension, $x_2^{(i)}$, from this space instead of from $\text{Unif}(R_2)$. This continues for all columns. In other words, progressive sampling uses the factorized model to steer the sampler into the high-mass part of the query region, compensating for the induced bias with importance weighting.

Example. We show the sampling procedure for a 3-filter query. Drawing the i -th sample for query $P(X_1 \in R_1, X_2 \in R_2, X_3 \in R_3)$:

1. Forward $\mathbf{0}$ to get $\hat{P}(X_1)$. Compute and store $\hat{P}(X_1 \in R_1)$ by summing. Then draw $x_1^{(i)} \sim \hat{P}(X_1|X_1 \in R_1)$.
2. Forward $x_1^{(i)}$ to get $\hat{P}(X_2|x_1^{(i)})$. Compute and store $\hat{P}(X_2 \in R_2|x_1^{(i)})$. Draw $x_2^{(i)} \sim \hat{P}(X_2|X_2 \in R_2, x_1^{(i)})$.
3. Forward $(x_1^{(i)}, x_2^{(i)})$ to get $\hat{P}(X_3|x_1^{(i)}, x_2^{(i)})$. Compute and store $\hat{P}(X_3 \in R_3|x_1^{(i)}, x_2^{(i)})$.

The summation and sampling steps are fast since they are only over single-column distributions. This is in contrast to integrating or summing over all columns at once, which has an exponential number of points. The product of the three stored intermediates,

$$\hat{P}(X_1 \in R_1) \cdot \hat{P}(X_2 \in R_2|x_1^{(i)}) \cdot \hat{P}(X_3 \in R_3|x_1^{(i)}, x_2^{(i)}) \quad (3)$$

is an unbiased estimate for the desired density. By construction, the sampled point satisfies the query ($x_1^{(i)}$ is drawn from range R_1 , $x_2^{(i)}$ from R_2 , and so forth). It remains to show that this sampler is approximating the correct sum:

THEOREM 1. *Progressive Sampling estimates are unbiased.*

The proof uses only basic probability rules and can be found in Appendix A. Algorithm 1 details the pseudocode for the general n -filter case. Note that when less than all columns are filtered, the unfiltered columns are treated as having a wildcard, i.e., $R_i = [0, D_i)$, and does not require special treatment. This sampler bears some resemblance to sequential importance sampling [10] and may be amenable

Algorithm 1 Progressive Sampling: estimate the density of query region $R_1 \times \dots \times R_n$ using S samples.

```

1: function PROGRESSIVESAMPLING( $S; R_1, \dots, R_n$ )
2:    $\hat{P} = 0$ 
3:   for  $i = 1$  to  $S$  do ▷ Batched in practice
4:      $\hat{P} = \hat{P} + \text{DRAW}(R_1, \dots, R_n)$ 
5:   return  $\hat{P}/S$ 

6: function DRAW( $R_1, \dots, R_n$ ) ▷ Draw one tuple
7:    $\hat{p} = 1$ 
8:    $\mathbf{s} = \mathbf{0}_n$  ▷ The tuple to fill in
9:   for  $i = 1$  to  $n$  do
10:    Forward pass through model:  $\mathcal{M}(\mathbf{s})$ 
11:     $\hat{P}(X_i|\mathbf{s}_{<i}) =$  the  $i$ -th model output ▷ Eq. 1
12:    Zero-out probabilities in slots  $[0, D_i) \setminus R_i$ 
13:    Re-normalize, obtaining  $\hat{P}(X_i|X_i \in R_i, \mathbf{s}_{<i})$ 
14:     $\hat{p} = \hat{p} \times \hat{P}(X_i \in R_i|\mathbf{s}_{<i})$ 
15:    Sample  $s_i \sim \hat{P}(X_i|X_i \in R_i, \mathbf{s}_{<i})$ 
16:     $\mathbf{s}[i] = s_i$ 
17:   return  $\hat{p}$  ▷ Density of the sampled tuple  $\mathbf{s}$ 

```

to applicable analysis. Progressive sampling has a sequential dependency between columns for drawing a single sample, but multiple samples can be drawn independently, which lends itself well for parallelization with modern hardware.

Lastly, we note that progressive sampling not only can operate on the model’s approximated joint, but Algorithm 1 also works on an oracle joint distribution (e.g., obtained by data scanning at each step). We take advantage of this observation in §6.7 to run the sampler against an oracle distribution. Our evaluation shows that the sampler can cover both low and high density regions, and handles challenging range queries for large numbers of columns and joint spaces.

6. EVALUATION

We answer the following questions in our evaluation:

1. How does Naru compare to state-of-the-art selectivity estimators in accuracy (§6.2)? Is it robust (§6.3)?
2. How long does it take to train a Naru model to achieve a useful level of accuracy? (§6.4)
3. Naru requires multiple inference passes to produce a selectivity estimate. How does this compare with the latency of other approaches? (§6.5)
4. How does accuracy scale with model size? (§6.6)
5. Lastly, a series of microbenchmarks are run to understand Naru’s limits (§6.7).

6.1 Experimental Setup

We compare Naru against predominant families of selectivity estimation techniques, including estimators in real databases, heuristics, non-parametric density estimators, and supervised learning approaches (Table 2). To ensure a fair comparison between estimators, we restrict each estimator to a fixed *storage budget* (Table 1). For example, for the Conviva-A dataset, Naru’s model must be less than 3MB in size, and the same restriction is held for all estimators for that dataset when applicable.

DATASET	ROWS	COLS	DOM.	JOINT	BUDGET
DMV	11.5M	11	2–2K	10^{15}	1.3% (13MB)
Conviva-A	4.1M	15	2–1.9K	10^{23}	0.7% (3MB)
Conviva-B	10K	100	2–10K	10^{190}	N/A

Table 1: **List of datasets used in evaluation.** “Dom.” refers to per-column domain size. “Joint” is number of entries in the exact joint distribution (equal to the product of all domain sizes). “Budget” is the storage budget we allocated to all evaluated estimators, when applicable, relative to the in-memory size of the corresponding original tables.

6.1.1 Datasets

We use real-world datasets (Table 1) with challenging characteristics. The number of rows ranges from 10K to 11.5M, the number of columns ranges from 11 to 100, and the size of the joint space ranges from 10^{15} to 10^{190} .

DMV [48]. Real-world dataset consisting of vehicle registration information in New York. We used the following 11 columns with widely differing dtypes and domain sizes (number in parenthesis indicates the domain size): `record_type` (4), `reg_class` (75), `state` (89), `county` (63), `body_type` (59), `fuel_type` (9), `valid_date` (2101), `color` (225), `sco_ind` (2), `sus_ind` (2), `rev_ind` (2). A total of 11,591,878 raw tuples are used. The exact joint distribution has a size of 3.4×10^{15} .

Conviva-A. Enterprise dataset containing anonymized user activity logs from a video analytics company. The table corresponds to 3 days of activities. The 15 columns contain a mix of small-domain categoricals (e.g., error flags, connection types) as well as large-domain numerical quantities (e.g., various bandwidth numbers in kbps). Although the domains have a range (2–1.9K) similar to DMV, there are many more numerical columns with larger domains, resulting in a much larger joint distribution (10^{23}).

Conviva-B. A small dataset of 10K rows and 100 columns also from Conviva, with a joint space of over 10^{190} . Though this dataset is trivial in size, this enables the use of an emulated, perfect-accuracy model for running detailed robustness studies (§6.7).

6.1.2 Estimators

Next, we discuss the baselines listed in Table 2, including the performed tunings.

Real databases. Postgres and DBMS-1 represent the performance a practitioner can hope to obtain from a real DBMS. Both rely on classical assumptions and 1D histograms, while the latter additionally contains cross-column correlation statistics. Every column has a histogram and associated statistics built. Postgres is tuned to use a maximum amount of per-column bins (10,000). For DBMS-1, one invocation of stats creation with all columns specified only builds a histogram on the first column; we therefore invoke stats creation several times so that all columns are covered.

Multi-dimensional histogram. Hist is our implementation of an N-dimensional histogram. We increase per-column bin sizes as much as possible to maximize its accuracy while staying within the space budget (otherwise it achieves perfect accuracy given unlimited space).

Independence assumption. Indep scans each column to obtain perfect per-column selectivities and combines them by multiplication. This measures the inaccuracy solely attributed to the independence assumption.

Kernel density estimators & Sampling. In the non-

TYPE	ESTIMATOR	DESCRIPTION
Histogram	Hist	N-dimensional histogram.
Heuristic	Indep	A baseline that multiplies <i>perfect</i> per-column selectivities.
Real System	Postgres	1D stats and histograms via independence/uniformity assumptions.
Real System	DBMS-1	Commercial DBMS: 1D stats plus inter-column unique value counts.
Sampling	Sample	Keeps $p\%$ of all tuples in memory. Estimates a new query by evaluating on those samples.
KDE	KDE	Kernel density estimation [19,21].
Prediction	MSCN	Supervised deep prediction net [25].
Deep L.M.	Naru	(Ours) Deep likelihood modeling.

Table 2: **List of estimators used in evaluation.**

parametric sampling regime, we evaluate a uniform sampler and a state-of-the-art KDE-based selectivity estimator [19,21]. Sample keeps a set of $p\%$ of tuples uniformly at random from the original table. In accordance with our memory budget for each dataset, p is set to 1.3% for DMV and 0.7% for Conviva-A. KDE [19] attempts to learn the underlying data distribution by averaging Gaussian kernels centered around random sample points. The number of sample points is chosen in accordance with our memory budget: 150K samples for DMV and 28K samples for Conviva-A. The bandwidth for KDE is computed via Scott’s rule [45]. The bandwidth for KDE-superv is initialized in the same way, but is further optimized through query feedback from 10K training queries. We modify the source code released by the authors [32] in order to run it with more than ten columns.

Supervised learning. We compare to a recently proposed supervised deep net-based estimator termed *multi-set convolutional network* [25], or MSCN. We apply the source code from the authors [1] to our datasets. As it is a *supervised* method, we generate 100K training queries from the same distribution the test queries are drawn, ensuring their “representativeness”. The net stores a materialized sample of the data. Every query is run on the sample to get a bitmap of qualifying tuples—this is used as an input additional to query features. We try three variants of the model, all with the same hyperparameters and all trained to convergence: MSCN-base uses the same setup reported originally [25] (1K samples, 100K training queries) and consumes 3MB. We found that MSCN’s performance is highly dependent on the samples, so we include a variant with $10\times$ more samples (MSCN-10K: 10K samples, 100K train queries), consuming 13MB (satisfying DMV’s budget only). We also include MSCN-0 which does not use any materialized samples and relies only on query features.

Deep likelihood modeling (ours). We train one Naru model for each dataset. All models are trained with the unsupervised maximum likelihood objective. For each dataset, the following model architectures are chosen by hand (§4.3) without automatic architecture search, and sizes are reported without any compression of network weights:

- DMV: masked multi-layer perceptron with 5 hidden layers (512, 256, 512, 128, 1024 units) consuming 12.7MB.
- Conviva-A: masked MLP with 4 hidden layers, 128 units each, consuming 2.7MB. Embedding reuse op-

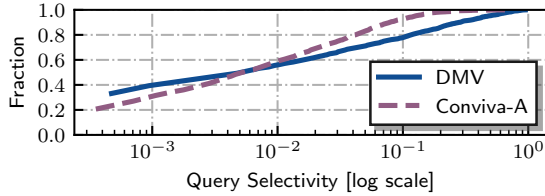


Figure 4: **Distribution of query selectivity** (§6.1.3).

timization with $h = 64$ is used (§4.2).

- Conviva-B: Emulated “oracle model”. This dataset is for microbenchmarks only.

For the timing experiments, we train and run the learning methods (KDE, MSCN, Naru) on a Tesla V100 GPU. Other estimators are run on an 8-core Intel E5-2686v4 2.30GHz machine and vectorized when applicable.

6.1.3 Workloads

Query distribution (Figure 4). We generate multidimensional queries containing both range and equality predicates. The goal is to test each estimator on a wide spectrum of target selectivities: we group them as high ($>2\%$), medium ($0.5\%–2\%$), and low ($\leq 0.5\%$). Intuitively, all solutions should perform reasonably well for high-selectivity queries, because dense regions require only coarse-grained modeling capacity. As the query selectivity drops, the estimation task becomes harder, since low-density regions require each estimator to model details in each hypercube. True selectivities are obtained by executing the queries on Postgres.

The query generator is inspired by prior work [25]. Instead of designating a few fixed columns to filter on, we consider the more challenging scenario where the filters are randomly placed. First, we draw the number of (non-wildcard) filters $5 \leq f \leq 11$ uniformly at random. We always include at least five filters to avoid queries with very high selectivity, which all estimators do similarly well at. Note that Naru’s progressive sampler treats non-filtered columns as having a wildcard filter, so it handles `num_cols` filters for each query. Next, f distinct columns are drawn to place the filters. For columns with domain size ≥ 10 , the filter operator is sampled uniformly from $\{=, \leq, \geq\}$; for columns with small domains, the equality operator is picked—the intention is to avoid placing a range predicate on categoricals, which often have a low domain size. The filter literals are then chosen from a random tuple sampled uniformly from the table (i.e., they follow the data distribution).

Overall, the generator proves expressive enough to yield the desired wide range of selectivities. Figure 4 shows the distribution of query selectivities of the generated queries (2,000 queries for each dataset).

Accuracy metric. We report accuracy by the multiplicative error [25,28,30] (also termed “q-error”), the factor by which an estimate differs from the actual cardinality:

$$\text{Error} := \max(\text{estimate}, \text{actual}) / \min(\text{estimate}, \text{actual})$$

We lower bound the estimated and actual cardinalities at 1 to guard against division by zero. In line with prior work [8,28], we found that the multiplicative error is much more informative than the *relative* error, as the latter does not fairly penalize small cardinality estimates (which are

frequently the case for high-dimensional queries). Lastly we report the errors in quantiles, with a particular focus at the tail. Our results show that all estimators can achieve low median (or mean) errors but with greatly varying performance at the tail, indicating that mean/median metrics do not accurately reflect the hard cases of the estimation task.

6.2 Estimation Accuracy

In summary, Tables 3 and 4 show that not only does Naru match or exceed the best estimator across the board, it excels in the *extreme tail of query difficulty*—that is, worst-case errors on low-selectivity queries. For these types of queries, Naru achieves orders of magnitude better accuracy than classical approaches, and at least $40\times$ better tail behavior than query-driven (supervised) methods.

The same Naru model is used to estimate all queries on a dataset, showing the robustness of the model learned. We now discuss these macrobenchmarks in more detail.

6.2.1 Results on DMV

Overall, Naru achieves the best accuracy and remains robust across the selectivity spectrum. Specifically, at tail, it is $230\times$ more accurate than DBMS-1, $94\times$ more accurate than Sample, $43\times$ more accurate than KDE-superv, and $230\times$ ($66\times$) more accurate than un-tuned (tuned) MSCN. We discuss several points of interest from Table 3:

Independence assumptions lead to order of magnitude errors. Estimators that assume full or partial independence between columns produce large errors, regardless of query selectivity or how good per-column estimates are. These include Hist, Indep, Postgres, and DBMS-1, whose tail errors are in the $10^3 – 10^5\times$ range. Naru’s model is powerful enough to avoid this assumption, leading to better results.

Worst-case errors are much harder to be robust against. All estimators perform worse for low-selectivity queries or at worst-case errors. For instance, in the high-selectivity regime Postgres’s error is a reasonable $1.55\times$ at 95th, but becomes $1682\times$ worse at the maximum. Also, Sample performs exceptionally well for high and medium selectivity queries, but drops off considerably for low selectivity queries where the sample has no hits. MSCN struggles since its supervised objective requires more training data to cover all possible low-selectivity queries. Naru makes much lower (single-digit) errors at the tail, showing the robustness that results from directly approximating the joint.

KDE struggles with high-dimensional data. KDE’s errors are among the highest. The reason is that, the bandwidth vector found is highly sub-optimal despite tunings, due to (1) a large number of attributes in DMV, and (2) discrete columns fundamentally do not work well with the notion of “distance” in KDE [19]. The method must rely on query feedback (KDE-superv) to find a good bandwidth.

MSCN heavily relies on its materialized data samples for accurate prediction. Across the spectrum, its accuracy closely approximates Sample. MSCN-10K has $3\times$ better tail accuracy than MSCN-base due to access to $10\times$ more samples, despite having the same network architecture and trained on the same 100K queries. Both variants’ accuracies drop off considerably for low-selectivity queries, since, when there are no hits in the materialized sample, the model relies solely on the query features to make “predictions”. MSCN-0 which does not use materialized samples performs considerably worse than the other two variants, obtaining a max

ESTIMATOR	HIGH ((2%, 100%])				MEDIUM ((0.5%, 2%])				Low ($\leq 0.5\%$)			
	Median	95th	99th	Max	Median	95th	99th	Max	Median	95th	99th	Max
Hist	$1 \cdot 10^4$	$4 \cdot 10^5$	$1 \cdot 10^6$	$2 \cdot 10^6$	$3 \cdot 10^4$	$2 \cdot 10^5$	$2 \cdot 10^5$	$2 \cdot 10^5$	$1 \cdot 10^3$	$3 \cdot 10^4$	$5 \cdot 10^4$	$6 \cdot 10^4$
Indep	1.12	1.55	46.14	2566	1.25	46.64	1051	$8 \cdot 10^4$	1.35	225.48	2231	$2 \cdot 10^4$
Postgres	1.12	1.55	46.26	2608	1.25	45.52	1070	$8 \cdot 10^4$	1.36	227.14	2287	$2 \cdot 10^4$
DBMS-1	1.45	3.36	5.80	12.60	2.72	6.38	9.29	10.10	5.28	83.00	416.75	917
Sample	1.00	1.02	1.03	1.05	1.02	1.05	1.07	1.10	1.12	43.20	98.08	377
KDE	10.92	1502	$1 \cdot 10^4$	$2 \cdot 10^5$	48.04	$2 \cdot 10^4$	$9 \cdot 10^4$	$2 \cdot 10^5$	38.00	3190.51	$2 \cdot 10^4$	$5 \cdot 10^4$
KDE-superv	1.40	3.81	4.91	13.32	1.53	4.36	8.12	16.94	1.95	30.00	98.04	175
MSCN-base	1.17	1.42	1.47	1.58	1.14	1.65	2.53	3.96	2.95	32.45	85.56	921
MSCN-0	16.77	92.38	194.64	285	8.89	80.43	343.64	471	4.79	67.13	169.09	6145
MSCN-10K	1.04	1.10	1.12	1.16	1.04	1.12	1.19	1.23	1.51	14.17	33.67	264
Naru-1000	1.01	1.03	1.08	1.34	1.02	1.08	1.20	1.44	1.04	1.53	2.43	17
Naru-2000	1.01	1.03	1.04	1.12	1.02	1.06	1.16	1.28	1.04	1.50	2.00	4

Table 3: **Estimation errors on DMV**. Errors are grouped by true selectivities and shown in percentiles computed from 2,000 queries.

ESTIMATOR	HIGH ((2%, 100%])				MEDIUM ((0.5%, 2%])				Low ($\leq 0.5\%$)			
	Median	95th	99th	Max	Median	95th	99th	Max	Median	95th	99th	Max
DBMS-1	1.75	5.25	7.77	9.12	3.93	13.61	19.88	31.28	8.63	176.22	636.01	4737
Sample	1.02	1.06	1.09	1.11	1.04	1.14	1.18	1.23	1.18	49.30	218.18	696
KDE	104.58	$2 \cdot 10^5$	$5 \cdot 10^5$	$8 \cdot 10^5$	346.82	$6 \cdot 10^4$	$8 \cdot 10^4$	$8 \cdot 10^4$	223.57	$1 \cdot 10^4$	$2 \cdot 10^4$	$2 \cdot 10^4$
KDE-superv	1.99	7.97	14.47	33.56	2.04	8.44	17.02	49.65	2.76	74.50	251.40	462
MSCN-base	1.14	1.27	1.36	1.48	1.15	1.55	2.26	57.71	2.05	20.33	84.12	370
Naru-1000	1.04	1.16	1.27	1.42	1.05	1.22	1.43	1.65	1.11	2.00	4.04	500
Naru-2000	1.03	1.12	1.19	1.25	1.05	1.17	1.24	1.30	1.09	1.78	4.00	54
Naru-4000	1.03	1.10	1.15	1.22	1.04	1.14	1.19	1.30	1.08	1.62	2.92	6

Table 4: **Estimation errors on Conviva-A**. Errors grouped by true selectivities and shown in percentiles computed from 2,000 queries.

error of $6145 \times$.

6.2.2 Results on Conviva-A

Based on DMV results, we keep only the promising baselines for this dataset. Table 4 shows that Naru remains best-in-class for a dataset with substantially different columns and a much larger joint size.

For this dataset, most estimators produce larger errors. This is because Conviva-A has a much larger joint space. DBMS-1 and KDE-superv exhibit $5 \times$ and $2.6 \times$ worse max error than before, respectively. MSCN-base’s max error in the medium-selectivity regime is also $14 \times$ worse. As a non-parametric method covering the full joint space, Sample remains a robust choice as the column count is scaled up.

For Naru, since the sampler need to cross more domains and a much larger joint space, Naru-1000 becomes insufficient to provide single-digit error in all cases. However, a modest scaling of the number of samples to 4K decreases the worst-case error back to single-digit levels. This suggests that the approximated joint is sufficiently accurate, and that the key challenge lies in *extracting its information*.

6.3 Robustness to Out of Distribution Queries

Our experiments thus far have drawn the filter literals (query centers) from the data. However, a strong estimator must be robust to out-of-distribution (OOD) queries where the literals are drawn from the entire joint domain, which often result in no matching tuples. Table 5 shows results on select estimators on 2K OOD queries on DMV, where 98% have a true cardinality of zero. The supervised MSCN-10K

suffers greatly (e.g., median is now $23 \times$, up from the $1.51 \times$ in Table 3) because it was trained on a set of in-distribution queries; at test time, out-of-distribution queries confuse the net. KDE-superv, a sampling-based approach, finds no hits in its sampled tuples, and therefore appropriately assigns zero density mass for all queries. This outlier-detection capability offered by KDEs has been studied [42].

ESTIMATOR	Median	95th	99th	Max
MSCN-10K	23	96	151	417
KDE-superv	1.00	1.00	3.67	163
Sample	1.00	1.00	2.00	116
Naru-2000	1.00	1.00	1.26	4.00

Table 5: Robustness to OOD queries. Errors from 2,000 queries.

Since Naru approximates the data distribution, it correctly learns that out-of-distribution regions have little or no density mass, outperforming KDE by $40 \times$ and MSCN by $104 \times$.

6.4 Training Time vs. Quality

Compared to supervised learning, Naru is efficient to train: no past queries are required; we only need access to a uniform random stream of tuples from the relation. We also find that, surprisingly, it only takes a few epochs of training to obtain a sufficiently powerful Naru estimator.

Figure 5 shows how two quality metrics, entropy gap and estimation error on the same workloads as before, change as training progresses. The metrics are calculated after each epoch (one pass over the data) finishes. An epoch takes about 75 seconds and 50 seconds for DMV and Conviva-A, respectively. The number of progressive samples is set to 2K

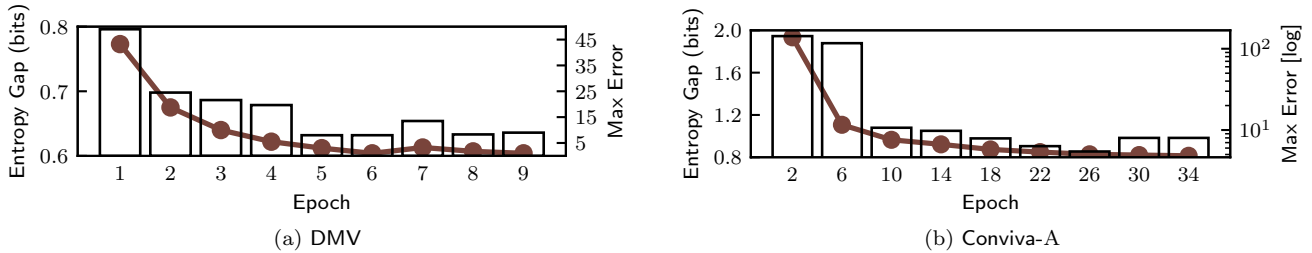


Figure 5: **Training time vs. quality** (§6.4). Dotted lines show divergence from data; bars show max estimation errors.

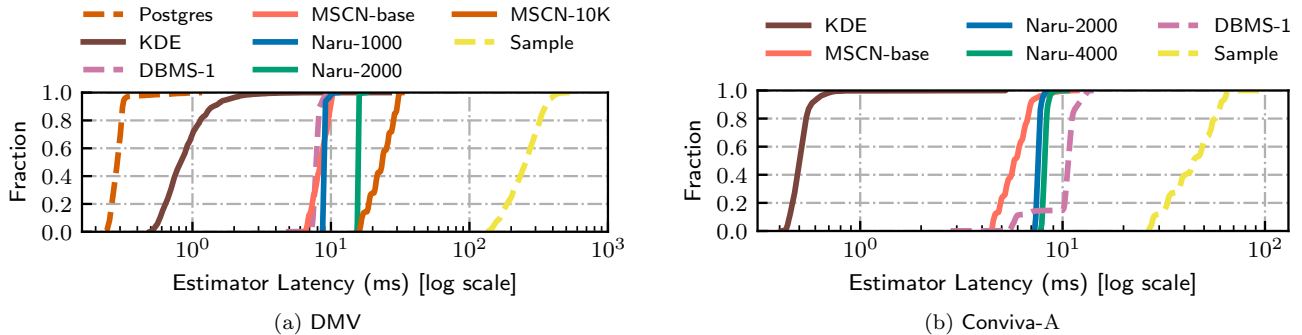


Figure 6: **Estimator latency** (§6.5). Learning methods are run on GPU; other estimators are run on CPU (dashed lines). Legend order follows line order; best viewed in color.

for DMV and 8K for Conviva-A.

Observe that **Naru** quickly converges to a high goodness-of-fit both in terms of entropy gap and estimation quality. For DMV where a larger **Naru** model is used, 1 epoch of training suffices to produce the best estimation accuracy compared to all baselines (Table 3, last column). For Conviva-A, 7 epochs yields the best-in-class quality and about 15 epochs yields the quality of single-digit max error.

6.5 Estimation Latency

As discussed in §5.1, **Naru**’s progressive sampling approach requires as many model forward passes as the number of attributes in the relation. In this section, we compare **Naru**’s estimation latency against other baselines. Figure 6 shows that, on our evaluation datasets, **Naru** can finish estimation in around 10ms on a GPU, which is much faster than scanning samples and is competitive with DBMS-1. We note the caveat that latencies for Postgres and DBMS-1 include producing an entire plan for each query. We further point out two observations.

First, a sizable gap exists between KDE and **Naru** (e.g., on DMV, 3ms vs. 10ms at 99%-tile). However, we note that while **Naru**’s sampler is written in Python code and a general-purpose deep learning framework (PyTorch), the former has hand-optimized GPU code (OpenCL). We believe the gap would shrink down if control logic overhead from Python is removed. Further, orthogonal techniques such as half-precision, i.e., 32-bit floats quantized into 16-bit floats, would shrink **Naru**’s compute cost by half.

Second, the CDF curves of most estimators are heavily slanted, indicating their latency being proportional to the number of attributes touched by the queries. **Naru** have upright curves because it treats all columns as having a filter—an unqueried column is treated as having a wildcard region.

Query region size. In addition, we compare the latency of **Naru**’s progressive sampling against the naive enumeration querying scheme discussed in §5. Table 6 shows, at the 99%-tile (with respect to the workload), (1) the query region size, or the number of points touched by each query, (2) the *estimated* latency for enumeration assuming peak GPU performance, and (3) the actual measured **Naru** latency, which uses progressive sampling. The results show that the naive enumeration querying scheme is impractical (>1000hr) compared to **Naru** (<=10ms) under the large query region sizes typical of real-world datasets.

	QUERY REGION	ENUM (est.)	Naru
DMV	$1.7 \cdot 10^{10}$	1111 hr	10ms
Conviva-A	$1.2 \cdot 10^{12}$	2777 hr	8ms

Table 6: Query region sizes vs. enumeration’s estimated per-query latency and **Naru**’s actual per-query latency, all at 99%-tile.

6.6 Choosing Model Size

In Table 7, we measure the relationship between model size and entropy gap on Conviva-A. While larger model sizes yield lower entropy gaps, Figure 5 shows that this can yield diminishing returns in terms of accuracy.

ARCHITECTURE	SIZE (MB)	Entropy gap, 5 epochs
$32 \times 32 \times 32 \times 32$	0.6	4.23 bits
$64 \times 64 \times 64 \times 64$	1.1	2.25 bits
$128 \times 128 \times 128 \times 128$	2.7	1.01 bits
$256 \times 256 \times 256 \times 256$	3.8	0.84 bits

Table 7: Larger model sizes yield lower entropy gap. Here we only consider scaling the number of units per hidden layer.

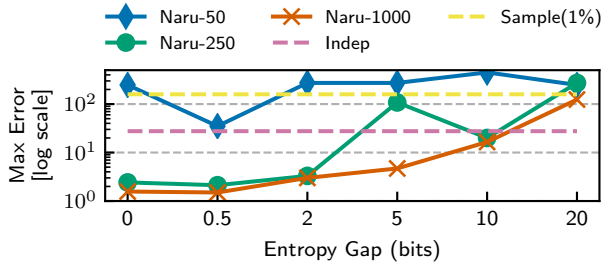


Figure 7: Accuracy of Naru as an artificial entropy gap is added to an oracle model for Conviva-B projected to the first 15 columns. 50 queries are drawn from the same distribution as in the macrobenchmarks. Naru has the best accuracy for an entropy gap of less than 2 bits, though remains competitive up to a surprisingly large gap of 10 bits. Variance of progressive sampling decreases dramatically when moving from 50 to 250 to 1000 samples.

6.7 Understanding Estimation Performance

Naru’s accuracy depends critically on two factors: (1) the accuracy of the density model; and (2) the effectiveness of progressive sampling. This section seeks to understand the interplay between the two components and how each contributes to estimation errors. We do this by running microbenchmarks against the Conviva-B dataset, which has only 10K rows but has 100 columns for a total joint space of 10^{190} . The small size of the dataset makes it possible to run queries against an emulated *oracle model* with perfect accuracy by scanning the data. This allows us to isolate errors introduced by density estimation vs. progressive sampling.

6.7.1 Robustness to Increasing Model Entropy Gap

One natural question is: how accurate does the density model have to be? One metric of modeling accuracy is *the fraction of total probability mass assigned to true data tuples*. For example, a randomly initialized model will assign equal probability mass to all points in the joint space of tuples. As training proceeds, it learns to assign higher probability to tuples actually present in the relation. Under the simplifying assumption that all relation tuples are unique (as they are in Conviva-B), we can quantify this fraction as follows. Suppose the model has an entropy gap of 2 bits; then, the fraction of probability mass assigned to the relation, f , satisfies $-\log_2 f = 2$, which leads to $f = 25\%$.

Figure 7 shows that Naru achieves the best performance with a model entropy gap of 0-2 bits. A gap of lower than 0.5 bits does not substantially improve performance. This means that for the best accuracy, the model must assign between 25 – 100% of the probability mass to the true data distribution. Surprisingly, Naru still outperforms baselines with up to 10 bits of entropy gap, which corresponds to less than $\approx 0.1\%$ probability mass assigned. We hypothesize the range queries makes such modeling errors less critical, because density errors of individual tuples could even out when estimating the density of the region as a whole.

6.7.2 Robustness to Increasing Column Counts

While the datasets tested in macrobenchmarks have a good number of columns, using Conviva-B we test how well progressive sampling scales to $10\times$ as many dimensions. One might suspect that, like many importance-sampling based approaches, progressive sampling has perhaps some exponential dependence on the number of columns, which would

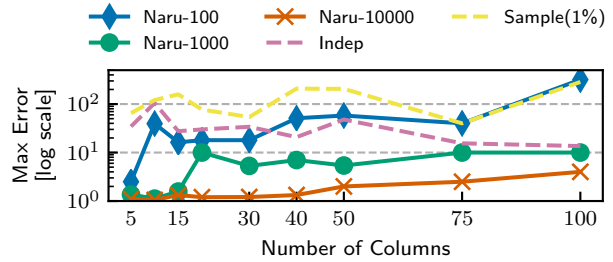


Figure 8: Accuracy of Naru as we add more columns from Conviva-B. We again use an oracle model (with 0 bits of entropy gap) and 50 randomly generated queries. The number of predicates covers at most 12 columns. The number of progressive sample paths required to accurately query the model increases modestly with the number of columns, but remains tractable even as the joint data space reaches over 10^{190} (at 100 columns).

prevent Naru from scaling to tables with many dozens of columns (e.g., of a multi-way joined relation).

Figure 8 shows that while the number of columns does significantly increase the variance of estimates, the number of progressive sample paths required to mitigate this variance remains tractable. A choice of 1000 sample paths produces reasonable worst-case accuracies for up to 100 columns, and 10000 sample paths improves on that by a modest factor.

There exist Monte Carlo integration techniques, e.g., the Metropolis-Hastings algorithm [35], that do not have a theoretical dependence on the number of dimensions. While these techniques typically have higher initial overheads, they are compatible with Naru and are worth exploring for scaling to many hundreds of columns or more.

6.7.3 Robustness to Data Shifts

Lastly, we study how Naru reacts to data shifts. We partition DMV by a date column into 5 parts. We then ingest each partition in order, emulating the common practice of “1 new partition per day”. Each estimator is built after seeing the first partition. After a new ingest, we test the previously-built estimators on queries that touch all data ingested so far. The same query generator as macrobenchmarks is used where the filters are drawn from tuples in the first partition (true selectivities computed on all data ingested so far).

PARTITIONS INGESTED	1	2	3	4	5
Naru, refreshed: max	2.0	2.0	2.0	2.0	2.0
90%-tile	1.20	1.14	1.12	1.14	1.15
Naru, stale: max	2.0	40.3	47.5	52.9	53.5
90%-tile	2.0	2.4	3.4	4.4	5.5

Table 8: Robustness to data shifts. Errors from 200 queries.

Table 8 shows the results of (1) Naru, no model updates, (2) Naru, with gradient updates on each new ingest. The model architecture is the same as in Table 3; 8,000 progressive samples are used since we are interested in learning how much imprecision or staleness presents in the model itself and not the effectiveness of information extraction. Results show that, Naru is able to handle queries on new data with reasonably good accuracy, even without having seen the new partitions. The model has learned to capture the underlying data correlations so the degradation is graceful.

7. RELATED WORK

Naru builds upon decades of rich research on selectivity estimation and this section cannot replace comprehensive surveys [7]. Below, we highlight the most related areas.

Joint approximation estimators. Multidimensional histograms [16,36,40,41] can be seen as coarse approximations to the joint data distribution. Probabilistic relational models (PRMs) [14] rely on a Bayes Net (conditional independence DAG) to factor the joint into materialized conditional probability tables. Tzoumas *et al.* [50] propose a variant of PRMs significantly optimized for practical use. Dependency-based histograms [8] make partial or conditional independence assumptions to keep the approximated joint tractable (factors stored as histograms). Concurrent work [17] also explores the use of deep likelihood models for selectivity estimation; they make straightforward application of these models for equality predicates, but provide no solution for range queries. Naru does not make *any* independence assumptions; it directly models the joint distribution and lazily encodes all chain-rule factors in a universal function approximator.

Query-driven estimators are supervised methods that take advantage of past or training queries [6]. ISOMER [47] and STHoles [4] are two representatives that adopt query feedback to improve histograms. LEO [49] and CardLearner [57] correct past statistics using feedback. QuickSel [38] recently pioneers a new query-driven histogram based on uniform mixture models. Heimes *et al.* [19] propose query-driven KDEs; Kiefer *et al.* [21] enhance them to handle joins. Deep learning regressors [31], e.g., MSCN [25], have also been proposed. Naru, an unsupervised data-driven synopsis, is orthogonal to this family. Our evaluation shows that our full joint approximation approach yields superior accuracy to two query-driven methods. However, the use of query feedback could serve as a beneficial fine-tuning mechanism.

ML in optimizers. Naru can be used as a drop-in replacement of selectivity estimator used in ML proposals to query optimization. Ortiz *et al.* [37] learns query representation to predict cardinalities, a discriminative (*prediction*) rather than our generative (*approximation*) approach. Neo [33], a *learned* query optimizer, approaches cardinality estimation *indirectly*: embeddings for all attribute values are first pre-trained; later, a value network uses them to encode predicate literals and additionally learns to correct or ignore signals from the embeddings. RL-based join optimizers (DQ [27], ReJOIN [34]) also use selectivities in their featurizations and may benefit from Naru’s estimates.

8. CONCLUSION

In conclusion, we believe that deep likelihood modeling is a promising approach for selectivity estimation. Modern high-capacity models allow us to accurately approximate the joint data distribution without independence assumptions. We contribute a novel Monte Carlo integration scheme that handles range predicates in addition to equalities over such models, which to the best of our knowledge has never been demonstrated. Our estimator, Naru, matches or exceeds state-of-the-art accuracy over several families of estimators.

Naru can be thought of as an unsupervised *neural synopsis*. In contrast to supervised learning-based estimators, Naru enjoys drastically more efficient training since there is no need to execute queries to collect feedback—it only needs to

read the data. Learning directly from the underlying data allows Naru to answer a much more general set of future queries and makes it inherently robust to shifts in the query workload. Our approach is non-intrusive and can serve as an opt-in component inside an optimizer.

A high-fidelity likelihood model trained on relation(s) may have other applications in data management. Outlier detection or data cleaning can benefit from a statistical model to check how likely a tuple is dirty [18] (i.e., outside the data distribution). Approximate query processing can *sample* in-distribution tuples from a compact synopsis, which may be much faster than sampling from the original storage. Data compression is also inherently linked to likelihood modeling. We leave exploring such uses of Naru to future investigation.

APPENDIX

A. PROOF OF THEOREM 1

PROOF. The proof uses only basic probability rules. For ease of exposition, we prove the 3-column case; the general N-column case follows the exact structure. Specifically, we need to show the expectation of Equation 3,

$$\mathbb{E}_{x_1^{(i)}, x_2^{(i)}} \left[\widehat{P}(X_3 \in R_3 | x_1^{(i)}, x_2^{(i)}) \widehat{P}(X_2 \in R_2 | x_1^{(i)}) \widehat{P}(X_1 \in R_1) \right]$$

equals the desired density. First, expanding the expectation over $x_1^{(i)}$ gives

$$\mathbb{E}_{x_2^{(i)}} \left[\sum_{x_1=K \in R_1} \widehat{P}(x_1 = K | x_1 \in R_1) \widehat{P}(X_3 \in R_3 | x_1 = K, x_2^{(i)}) \widehat{P}(X_2 \in R_2 | x_1 = K) \widehat{P}(X_1 \in R_1) \right]$$

Applying Bayes’ rule to the new conditional term,

$$\mathbb{E}_{x_2^{(i)}} \left[\sum_{x_1=K \in R_1} \frac{\widehat{P}(x_1 = K)}{\widehat{P}(X_1 \in R_1)} \widehat{P}(X_3 \in R_3 | x_1 = K, x_2^{(i)}) \widehat{P}(X_2 \in R_2 | x_1 = K) \widehat{P}(X_1 \in R_1) \right]$$

Similarly, we expand the expectation over $x_2^{(i)}$ and applying the same rule to get

$$\sum_{\substack{x_1=K \in R_1 \\ x_2=M \in R_2}} \left[\frac{\widehat{P}(x_2 = M | x_1 = K)}{\widehat{P}(X_2 \in R_2 | x_1 = K)} \frac{\widehat{P}(x_1 = K)}{\widehat{P}(X_1 \in R_1)} \widehat{P}(X_3 \in R_3 | x_1 = K, x_2 = M) \widehat{P}(X_2 \in R_2 | x_1 = K) \widehat{P}(X_1 \in R_1) \right]$$

Canceling terms, we obtain

$$\sum_{\substack{x_1=K \in R_1 \\ x_2=M \in R_2}} \left[\widehat{P}(X_3 \in R_3 | x_1 = K, x_2 = M) \widehat{P}(x_2 = M | x_1 = K) \widehat{P}(x_1 = K) \right]$$

which is the density $\widehat{P}(X_1 \in R_1, X_2 \in R_2, X_3 \in R_3)$. \square

2. REFERENCES

- [1] A. Kipf. Github repository, learnedcardinalities. github.com/andreaskipf/learnedcardinalities, 2019. [Online; accessed March, 2019].
- [2] S. Agarwal, H. Milner, A. Kleiner, A. Talwalkar, M. Jordan, S. Madden, B. Mozafari, and I. Stoica. Knowing when you're wrong: building fast and reliable approximate query processing systems. In *Proceedings of the 2014 ACM SIGMOD international conference on Management of data*, pages 481–492. ACM, 2014.
- [3] M. Akdere, U. Çetintemel, M. Riondato, E. Upfal, and S. B. Zdonik. Learning-based query performance modeling and prediction. In *2012 IEEE 28th International Conference on Data Engineering*, pages 390–401. IEEE, 2012.
- [4] N. Bruno, S. Chaudhuri, and L. Gravano. Stholes: A multidimensional workload-aware histogram. In *Proceedings of the 2001 ACM SIGMOD International Conference on Management of Data*, SIGMOD '01, pages 211–222, New York, NY, USA, 2001. ACM.
- [5] S. Chaudhuri, R. Motwani, and V. Narasayya. On random sampling over joins. In *ACM SIGMOD Record*, volume 28, pages 263–274. ACM, 1999.
- [6] C. M. Chen and N. Roussopoulos. Adaptive selectivity estimation using query feedback. In *Proceedings of the 1994 ACM SIGMOD International Conference on Management of Data*, SIGMOD '94, pages 161–172, New York, NY, USA, 1994. ACM.
- [7] G. Cormode, M. Garofalakis, P. J. Haas, and C. Jermaine. Synopses for massive data: Samples, histograms, wavelets, sketches. *Foundations and Trends in Databases*, 4(1–3):1–294, 2011.
- [8] A. Deshpande, M. Garofalakis, and R. Rastogi. Independence is good: Dependency-based histogram synopses for high-dimensional data. *ACM SIGMOD Record*, 30(2):199–210, 2001.
- [9] L. Dinh, J. Sohl-Dickstein, and S. Bengio. Density estimation using real NVP. In *5th International Conference on Learning Representations, ICLR 2017, Toulon, France, April 24–26, 2017, Conference Track Proceedings*, 2017.
- [10] A. Doucet, N. De Freitas, and N. Gordon. An introduction to sequential monte carlo methods. In *Sequential Monte Carlo methods in practice*, pages 3–14. Springer, 2001.
- [11] J. Friedman, T. Hastie, and R. Tibshirani. *The elements of statistical learning*. Springer series in statistics New York, 2001.
- [12] M. Germain, K. Gregor, I. Murray, and H. Larochelle. Made: Masked autoencoder for distribution estimation. In *International Conference on Machine Learning*, pages 881–889, 2015.
- [13] L. Getoor, N. Friedman, D. Koller, and B. Taskar. Learning probabilistic models of relational structure. In *ICML*, volume 1, pages 170–177, 2001.
- [14] L. Getoor, B. Taskar, and D. Koller. Selectivity estimation using probabilistic models. In *ACM SIGMOD Record*, volume 30, pages 461–472. ACM, 2001.
- [15] G. Grimmett, D. Stirzaker, et al. *Probability and random processes*. Oxford university press, 2001.
- [16] D. Gunopulos, G. Kollios, V. J. Tsotras, and C. Domeniconi. Selectivity estimators for multidimensional range queries over real attributes. *The VLDB Journal*, 14(2):137–154, 2005.
- [17] S. Hasan, S. Thirumuruganathan, J. Augustine, N. Koudas, and G. Das. Multi-attribute selectivity estimation using deep learning. *arXiv preprint arXiv:1903.09999*, 2019.
- [18] A. Heidari, J. McGrath, I. F. Ilyas, and T. Rekatsinas. HoloDetect: Few-shot learning for error detection. In *Proceedings of the 2019 ACM SIGMOD international conference on Management of data*. ACM, 2019.
- [19] M. Heimel, M. Kiefer, and V. Markl. Self-tuning, gpu-accelerated kernel density models for multidimensional selectivity estimation. In *Proceedings of the 2015 ACM SIGMOD International Conference on Management of Data*, SIGMOD '15, pages 1477–1492, New York, NY, USA, 2015. ACM.
- [20] R. Kaushik, J. F. Naughton, R. Ramakrishnan, and V. T. Chakravarthy. Synopses for query optimization: A space-complexity perspective. volume 30, pages 1102–1127, New York, NY, USA, Dec. 2005. ACM.
- [21] M. Kiefer, M. Heimel, S. Breß, and V. Markl. Estimating join selectivities using bandwidth-optimized kernel density models. *Proceedings of the VLDB Endowment*, 10(13):2085–2096, 2017.
- [22] D. P. Kingma and J. Ba. Adam: A method for stochastic optimization. In *3rd International Conference on Learning Representations, ICLR 2015, San Diego, CA, USA, May 7–9, 2015, Conference Track Proceedings*, 2015.
- [23] D. P. Kingma and P. Dhariwal. Glow: Generative flow with invertible 1x1 convolutions. In *Advances in Neural Information Processing Systems*, pages 10215–10224, 2018.
- [24] D. P. Kingma and M. Welling. Auto-encoding variational bayes. In *2nd International Conference on Learning Representations, ICLR 2014, Banff, AB, Canada, April 14–16, 2014, Conference Track Proceedings*, 2014.
- [25] A. Kipf, T. Kipf, B. Radke, V. Leis, P. A. Boncz, and A. Kemper. Learned cardinalities: Estimating correlated joins with deep learning. In *CIDR 2019, 9th Biennial Conference on Innovative Data Systems Research, Asilomar, CA, USA, January 13–16, 2019*.
- [26] F. Korn, T. Johnson, and H. Jagadish. Range selectivity estimation for continuous attributes. In *Proceedings. Eleventh International Conference on Scientific and Statistical Database Management*, pages 244–253. IEEE, 1999.
- [27] S. Krishnan, Z. Yang, K. Goldberg, J. Hellerstein, and I. Stoica. Learning to optimize join queries with deep reinforcement learning. *arXiv preprint arXiv:1808.03196*, 2018.
- [28] V. Leis, A. Gubichev, A. Mirchev, P. Boncz, A. Kemper, and T. Neumann. How good are query optimizers, really? *Proceedings of the VLDB Endowment*, 9(3):204–215, 2015.
- [29] V. Leis, B. Radke, A. Gubichev, A. Kemper, and T. Neumann. Cardinality estimation done right: Index-based join sampling. In *CIDR*, 2017.
- [30] V. Leis, B. Radke, A. Gubichev, A. Mirchev, P. Boncz, A. Kemper, and T. Neumann. Query optimization through the looking glass, and what we found running the join order benchmark. *The VLDB Journal*, pages 1–26, 2018.
- [31] H. Liu, M. Xu, Z. Yu, V. Corvinelli, and C. Zuzarte. Cardinality estimation using neural networks. In *Proceedings of the 25th Annual International Conference on Computer Science and Software Engineering*, pages 53–59. IBM Corp., 2015.
- [32] M. Heimel. Bitbucket repository, feedback-kde. bitbucket.org/mheimel/feedback-kde, 2019. [Online; accessed March, 2019].
- [33] R. Marcus, P. Negi, H. Mao, C. Zhang, M. Alizadeh, T. Kraska, O. Papaemmanouil, and N. Tatbul. Neo: A learned query optimizer. *arXiv preprint arXiv:1904.03711*, 2019.
- [34] R. Marcus and O. Papaemmanouil. Deep reinforcement learning for join order enumeration. In *Proceedings of the First International Workshop on Exploiting Artificial Intelligence Techniques for Data Management, aiDM'18*, pages 3:1–3:4, New York, NY, USA, 2018. ACM.
- [35] M. Mitzenmacher and E. Upfal. *Probability and computing: Randomization and probabilistic techniques in algorithms and data analysis*. Cambridge university press, 2017.
- [36] M. Muralikrishna and D. J. DeWitt. Equi-depth multidimensional histograms. In *ACM SIGMOD Record*, volume 17, pages 28–36. ACM, 1988.
- [37] J. Ortiz, M. Balazinska, J. Gehrke, and S. S. Keerthi. Learning state representations for query optimization with deep reinforcement learning. *CoRR*, 2018.

- [38] Y. Park, S. Zhong, and B. Mozafari. Quicksel: Quick selectivity learning with mixture models. *arXiv preprint arXiv:1812.10568*, 2018.
- [39] M. Perron, Z. Shang, T. Kraska, and M. Stonebraker. How i learned to stop worrying and love re-optimization. In *35th IEEE International Conference on Data Engineering, ICDE 2019*, 2019.
- [40] V. Poosala, P. J. Haas, Y. E. Ioannidis, and E. J. Shekita. Improved histograms for selectivity estimation of range predicates. In *Proceedings of the 1996 ACM SIGMOD International Conference on Management of Data, SIGMOD '96*, pages 294–305, New York, NY, USA, 1996. ACM.
- [41] V. Poosala and Y. E. Ioannidis. Selectivity estimation without the attribute value independence assumption. In *VLDB*, volume 97, pages 486–495, 1997.
- [42] X. Qin, L. Cao, E. A. Rundensteiner, and S. Madden. Scalable kernel density estimation-based local outlier detection over large data streams. In *22nd International Conference on Extending Database Technology, EDBT 2019*, 2019.
- [43] A. Radford, J. Wu, R. Child, D. Luan, D. Amodei, and I. Sutskever. Language models are unsupervised multitask learners. URL <https://openai.com/blog/better-language-models>, 2019.
- [44] T. Salimans, A. Karpathy, X. Chen, and D. P. Kingma. Pixelcnn++: Improving the pixelcnn with discretized logistic mixture likelihood and other modifications. In *5th International Conference on Learning Representations, ICLR 2017, Toulon, France, April 24-26, 2017, Conference Track Proceedings*, 2017.
- [45] D. W. Scott. *Multivariate Density Estimation: Theory, Practice, and Visualization*. John Wiley & Sons, Inc., 1992.
- [46] P. G. Selinger, M. M. Astrahan, D. D. Chamberlin, R. A. Lorie, and T. G. Price. Access path selection in a relational database management system. In *Proceedings of the 1979 ACM SIGMOD international conference on Management of data*, pages 23–34. ACM, 1979.
- [47] U. Srivastava, P. J. Haas, V. Markl, M. Kutsch, and T. M. Tran. Isomer: Consistent histogram construction using query feedback. In *22nd International Conference on Data Engineering (ICDE'06)*, pages 39–39. IEEE, 2006.
- [48] State of New York. Vehicle, snowmobile, and boat registrations. catalog.data.gov/dataset/vehicle-snowmobile-and-boat-registrations, 2019. [Online; accessed March 1st, 2019].
- [49] M. Stillger, G. M. Lohman, V. Markl, and M. Kandil. Leo-db2's learning optimizer. In *VLDB*, volume 1, pages 19–28, 2001.
- [50] K. Tzoumas, A. Deshpande, and C. S. Jensen. Lightweight graphical models for selectivity estimation without independence assumptions. *Proceedings of the VLDB Endowment*, 4(11):852–863, 2011.
- [51] B. Uria, I. Murray, and H. Larochelle. A deep and tractable density estimator. *CoRR*, 2013.
- [52] A. van den Oord, S. Dieleman, H. Zen, K. Simonyan, O. Vinyals, A. Graves, N. Kalchbrenner, A. Senior, and K. Kavukcuoglu. Wavenet: A generative model for raw audio. In *Arxiv*, 2016.
- [53] A. Van den Oord, N. Kalchbrenner, L. Espeholt, O. Vinyals, A. Graves, et al. Conditional image generation with pixelcnn decoders. In *Advances in neural information processing systems*, pages 4790–4798, 2016.
- [54] A. Vaswani, N. Shazeer, N. Parmar, J. Uszkoreit, L. Jones, A. N. Gomez, L. Kaiser, and I. Polosukhin. Attention is all you need. In *Advances in neural information processing systems*, pages 5998–6008, 2017.
- [55] T. L. Veldhuizen. Triejoin: A simple, worst-case optimal join algorithm. In *ICDT*, 2014.
- [56] S. D. Viglas, J. F. Naughton, and J. Burger. Maximizing the output rate of multi-way join queries over streaming information sources. In *Proceedings of the 29th international conference on Very large data bases-Volume 29*, pages 285–296. VLDB Endowment, 2003.
- [57] C. Wu, A. Jindal, S. Amizadeh, H. Patel, W. Le, S. Qiao, and S. Rao. Towards a learning optimizer for shared clouds. *Proc. VLDB Endow.*, 12(3):210–222, Nov. 2018.